Atmos. Chem. Phys. Discuss., https://doi.org/10.5194/acp-2017-678
Manuscript under review for journal Atmos. Chem. Phys.
Discussion started: 26 July 2017

Atmospheric Chemistry and Physics Discussions

High-resolution quantification of atmospheric CO_2 mixing ratios in the Greater Toronto Area, Canada

Stephanie C. Pugliese[1], Jennifer G. Murphy[1*], Felix R. Vogel[2,4], Michael D. Moran[3], Junhua Zhang[3], Qiong Zheng[3], Craig A. Stroud[3], Shuzhan Ren[3], Douglas Worthy[4], Gregoire Broquet[2]

[1] University of Toronto, Department of Chemistry, 80 St. George St, Toronto, ON, Canada M5S 3H6

[2] Laboratoire des Sciences du Climat et de L'Environnement, CEA-CNRS-UVSQ, Université de Paris-Saclay, France

[3] Environment Canada, Air Quality Research Division, 4905 Dufferin St. Toronto, ON, Canada M3H 5T4

[4] Environment Canada, Climate Research Division, 4905 Dufferin St. Toronto, ON, Canada M3H 5T4

*Correspondence author. Email address: jmurphy@chem.utoronto.ca (J.G. Murphy)

Atmos. Chem. Phys. Discuss., https://doi.org/10.5194/acp-2017-678
Manuscript under review for journal Atmos. Chem. Phys.
Discussion started: 26 July 2017

Atmospheric Chemistry and Physics Discussions

Abstract

Many stakeholders are seeking methods to reduce carbon dioxide (CO_2) emissions in urban areas, however reliable, high-resolution inventories are required to guide these efforts. We present the development of a high-resolution CO_2 inventory available for the Greater Toronto Area and surrounding region in southern Ontario, Canada (area of ~2.8 x 10^5 km^2, 26 % of the province of Ontario). The new SOCE (Southern Ontario CO_2 Emissions) inventory is available at the 2.5 x 2.5 km spatial and hourly temporal resolution and characterizes emissions from seven sectors: Area, Residential natural gas combustion, Commercial natural gas combustion, Point, Marine, On-road and Off-road. To assess the accuracy of the SOCE inventory, we developed an observation-model framework using the GEM-MACH chemistry-transport model run on a high-resolution grid with 2.5 km grid spacing coupled to the Fossil Fuel Data Assimilation System (FFDAS) v2 inventories for anthropogenic CO_2 emissions and the European Center for Medium-Range Weather Forecasts (ECMWF) land carbon model C-TESSEL for biogenic fluxes. A run using FFDAS v2 for the southern Ontario region was compared to a run in which its emissions were replaced by the SOCE inventory. Simulated CO_2 mixing ratios were compared against in situ measurements made at four sites in southern Ontario, Downsview, Hanlan's Point, Egbert and Turkey Point, in three winter months, January-March, 2016. Model simulations had better agreement with measurements when using the SOCE inventory emissions versus other inventories, quantified using a variety of statistics such as correlation coefficient, root mean square error and mean bias. Furthermore, when run with the SOCE inventory, the model had improved ability to capture the typical diurnal pattern of CO_2 mixing ratios, particularly at the Downsview, Hanlan's Point and Egbert sites. In addition to improved model-measurement agreement, the SOCE inventory offers a sectoral breakdown of emissions, allowing estimation of average time-of-day and day-of-week contributions of different sectors. Our results show that at night, emissions from Residential and Commercial natural gas combustion and other

Area sources can contribute > 80 % of the CO_2 enhancement while during the day emissions from the On-road sector dominate, accounting for >70 % of the enhancement.

1.0 Introduction

Urban areas are sites of dense population and the intensity of human activities (such as transportation, industry and residential and commercial development) makes them hot-spots for anthropogenic carbon dioxide (CO_2) emissions. While occupying only 3 % of the total land area, urban areas are locations of residence for 54 % of the global population and are the source of 53 – 87 % of anthropogenic CO_2 emissions globally (IPCC-WG3, 2014; WHO, 2015). When considering Canada alone, the urban population accounts for an even larger fraction of the total (81 % in 2011) (Statistics Canada, 2011) while urban areas cover only 0.25 % of the land area (Statistics Canada, 2009). Recognizing their influence on the global carbon budget, many urban areas are seeking methods to reduce their anthropogenic CO_2 emissions. The Greater Toronto Area (GTA) in southeastern Canada, for example, has committed to the *Change is in the Air* initiative as well as being a part of the *C40 Cities Climate Leadership Group,* both of which call to reduce CO_2 emissions 30 % below 1990 levels by 2020 (C40 Cities, 2016; Framework for Public Review and Engagement, 2007). However, in order to effectively guide anthropogenic CO_2 mitigation strategies, reliable inventories are needed, particularly at high spatial and temporal resolution, to gain a better understanding of the carbon cycle (Gurney et al., 2009; Patarasuk et al., 2016). To our knowledge, the only spatially disaggregated CO_2 inventories available for use in the GTA are the EDGAR v.4.2 (Emission Database for Global Atmospheric Research) CO_2 inventory (available at annual, 0.1^o x 0.1^o resolution) (EDGAR, 2010) and the FFDAS v2 (Fossil Fuel Data Assimilation System) CO_2 inventory (available at hourly, 0.1^o x 0.1^o resolution) (FFDAS, 2010), both which are limited in their spatial and/or temporal resolution and therefore are not well-suited for the quantification and understanding of CO_2 emissions at the urban

scale. The Canadian national CO_2 inventory, on the other hand, is only available at the provincial level (Environment Canada, 2012).

Efforts to develop emission inventories at the fine spatial and temporal resolution required for urban-scale understanding of CO_2 emissions has been driven both by policy- and science-related questions (Gurney et al., 2009; Patarasuk et al., 2016). From a policy perspective, improving CO_2 emission quantification is essential to independently evaluate whether anthropogenic mitigation regulations are being effectively implemented. From a scientific perspective, gaining information about anthropogenic CO_2 emissions from urban areas has been primarily motivated by atmospheric CO_2 inversions, which are used to better understand the global carbon cycle (Gurney et al., 2009; Patarasuk et al., 2016). Regardless of the motivation, quantification of CO_2 source/sink processes currently uses two techniques: the bottom-up approach and the top-down approach. In the bottom-up approach, local-scale activity level information is combined with appropriate emission factors to infer emission rates. This method has been used widely to develop many inventories (EDGAR, 2010; FFDAS, 2010; Gurney et al., 2009) but is limited by the accuracy of the input parameters. Conversely, in the top-down approach, inverse modelling is used to exploit the variability in atmospheric mixing ratios of CO_2 to identify the source/sink distributions and magnitudes; this method is limited by insufficient mixing ratio data and uncertainties in simulating atmospheric transport (Pillai et al., 2011). Given current policy needs, a strategy using solely bottom-up or top-down approaches is likely insufficient to evaluate CO_2 emissions but rather a synthesis of the two methodologies is required (Miller and Michalak, 2016). Successful examples of high-resolution CO_2 inventory development are available on the urban scale, such as the Airparif inventory in Ile-de-France (publicly available at http://www.airparif.asso.fr/en/index/index) and in Indianapolis, Los Angeles, Salt Lake City and Phoenix through the Hestia project (Gurney et al., 2012), on the national scale, such as in China (Zhao et al., 2012), and on the global scale (Wang et al., 2013). However, to our knowledge, there are

currently no studies that have quantified Canadian CO_2 emissions at the fine spatial and temporal resolution required for urban analyses in Canada.

In an effort to address this gap, this study was focused on quantifying CO_2 emissions at a fine spatial and temporal resolution in the GTA and southern Ontario (we expanded the inventory beyond the urban area of the GTA so we could exploit information on CO_2 mixing ratios collected at rural areas in central and south-western Ontario, proving additional sites for inventory validation). We present the new high-resolution Southern Ontario CO_2 Emissions (SOCE) inventory, which quantifies CO_2 emissions from seven source sectors (On-road, Off-road, Area, Point, Marine, Residential, and Commercial natural gas combustion) at 2.5 km x 2.5 km spatial and hourly temporal resolution for an area covering ~26 % of the province of Ontario (~2.8×10^5 km^2). The SOCE inventory was used in combination with the Environment and Climate Change Canada (ECCC) GEM-MACH chemistry-transport model to simulate CO_2 mixing ratios in a domain including south-eastern Canada and the northeastern USA (hereafter referred to as the "PanAm domain") for comparison with in situ measurements made by the Southern Ontario Greenhouse Gas Network. Until now, estimates of anthropogenic CO_2 emissions in the GTA were available only from the EDGAR v.4.2 (EDGAR, 2010) and the FFDAS v2 (FFDAS, 2010) inventories, which have very different annual totals for this region (1.36×10^8 vs. 1.05×10^8 tonnes CO_2, respectively). Therefore, we expect the results of this work will improve our ability to quantify the emissions of CO_2 in the entire domain as well as the relative contributions of different sectors, providing a more detailed characterization of the carbon budget in the GTA.

2.0 Methods

2.1 Geographic Domain

The geographic focus of this study was the GTA in southern Ontario, Canada. The GTA is the largest urban area in Canada; it comprises five municipalities, Toronto, Halton, Durham, Peel and York,

which together have a population exceeding 6 million (Statistics Canada., 2012b). Although the GTA comprises only 0.07 % of Canadian land area, it represents over 17 % of the total population as a result of rapid urbanization over the past few decades (Statistics Canada., 2012b). Therefore, high-resolution characterization of CO_2 emissions can help integrate climate policy with urban planning. This region is home to a network of measurement sites providing long-term, publicly available datasets of atmospheric CO_2 mixing ratio measurements, *Sect. 2.2* (Environment Canada, 2011) which can be used to evaluate model outputs and inventory estimates. In 2016 the government of Ontario released a Climate Change Action Plan, which includes an endowment given to the Toronto Atmospheric Fund of $17 million to invest in strategies to reduce greenhouse gas pollution in the GTA (Ontario, 2016). Therefore this research can provide timely information on the carbon budget in the GTA and help to implement effective reduction strategies.

2.2 The Southern Ontario Greenhouse Gas Network

Measurements of ambient CO_2 dry air mixing ratios began in 2005 in southern Ontario at the Egbert station followed by the Downsview station (2007), Turkey Point station (2012) and Hanlan's Point station (2014), Figure 1. Egbert is located ~75 km north-northwest of Toronto in a rural area, Downsview is located ~20 km north of downtown core of the city of Toronto in a populated suburban area, Turkey Point is located to the south-west of the GTA in a rural area on the north shore of Lake Erie, and Hanlan's Point is located on Toronto Island, just south of the city of Toronto on the shore of Lake Ontario. Site details and instrument types used can be found in Table 1. CO_2 measurements are collected as a part of ECCC's Greenhouse Gas Observational Program. The measurement procedure follows a set of established principles and protocols outlined by a number of international agencies through recommendations of the *Meeting on Carbon Dioxide, Other Greenhouse Gases, and Related Measurement Techniques,* coordinated by the World Meteorological Organization (WMO) every 2 years.

The atmospheric CO_2 observational program Egbert is based on non-dispersive infrared (NDIR) methodology and fine-tuned for high precision measurements (Worthy et al., 2005). A detailed description of the NDIR observational system can be found in Worthy et al, (2005). The atmospheric CO_2 observational programs at Turkey Point, Downsview, and Hanlan's Point are based on Cavity Ring-Down Spectrometer (CRDS). Each Picarro CRDS system is calibrated in the ECCC central calibration facility in Toronto before deployment to the field. The response function of the analyzer is determined against 3 calibrated standards tanks (Low, Mid, High). The working (W) and target (T) tanks assigned to the system are also included in the injection sequence and calibrated. At each site, ambient measurements are made using two sample lines placed at the same level. Each sample line has separate dedicated sample pumps and driers (~ -30°C). Pressurized aluminum 30 L gas cylinders are used for the working and target tanks. The sample flow rate of the ambient and standard tank gases is set at ~300 cc/min. The injection sequence consists of a target and working tanks sequentially passed through the analyzer for 10 minutes each every 2 days. The ambient data from line1 is passed through the analyzer for 18 hours followed by Line2 for 6 hours. The Line1/Line2 sequence repeats one time before the target and working tanks are again passed through the system. The working and target tanks are calibrated on site at least once per year against a single transfer standard transported between the sites and the central laboratory facility in Toronto. The CO_2 measurements from both the NDIR and CRDS analytical systems have a precision of around 0.1 ppm based on one-minute averages and are accurate to within 0.2 ppm.

2.3 GEM-MACH chemistry- transport model

In this project, we used the GEM-MACH (Global Environmental Multi-scale–Modelling Air quality and CHemistry) chemistry–transport model (CTM) (Gong et al., 2015; Moran et al., 2013; Pavlovic et al., 2016; Talbot et al., 2008) to link surface emission estimates and atmospheric mixing ratios. GEM-MACH is an on–line CTM embedded within the Canadian weather forecast model GEM (Côté et al.,

1998a; Côté et al., 1998b). The configuration of GEM-MACH used in our study has 62 vertical levels from the surface to ~1.45 hPa on a terrain-following staggered vertical grid for a log-hydrostatic pressure coordinate. The thickness of the lowest layer was 40 m. The PanAm domain used in our simulations, which includes central and southern Ontario, as well as western Quebec and the northeastern USA, is shown in Figure 1. The PanAm domain has 524 x 424 grid cells in the horizontal on a rotated latitude-longitude grid with 2.5-km grid spacing and covers an area of approximately 1310 km x 1060 km (total domain area is 1.39 x 10^6 km^2). A 24-hour forecasting period was used with a 60-second time step for each integration cycle. Meteorological fields (wind, temperature, humidity, etc.) were re-initialized every 24 hours (i.e., after each model integration cycle); chemical fields were carried forward from the previous integration cycle (i.e., perpetual forecast). Hourly meteorological and chemical boundary conditions were provided by the ECCC operational 10-km GEM-MACH air quality forecast model (Moran et al., 2015).

In our study, we simulated two scenarios of CO_2 surface fluxes, indicated by the sum of the following:

Scenario 1:

- Anthropogenic fossil fuel CO_2 emissions within the province of Ontario estimated by the SOCE inventory, available at 2.5 km x 2.5 km spatial and hourly temporal resolution, as described in *Sect. 2.4*
- Anthropogenic fossil fuel CO_2 emissions estimated by the FFDAS v2 inventory (FFDAS, 2010) outside of the province of Ontario (province of Quebec and USA), available at 0.1° x 0.1° spatial and hourly temporal resolution
- Biogenic CO_2 fluxes from the C-TESSEL land surface model, as described in *Sect. 2.5*

Scenario 2:

- Anthropogenic fossil fuel CO_2 emissions estimated by the FFDAS v2 inventory (FFDAS, 2010) for the entire domain, available at 0.1° x 0.1° spatial and hourly temporal resolution
- Biogenic CO_2 fluxes from the C-TESSEL land surface model, as described in *Sect. 2.5*

CO_2 is not a usual chemical species considered by GEM-MACH but a set of special inert tracer fields were added to GEM-MACH for this project to account for CO_2 concentration fields associated with difference source sectors and the lateral boundaries. The CO_2 boundary conditions set at the lateral and top edges of the domain were obtained from the Monitoring Atmospheric Composition and Climate (MACC) global inversion, v.10.2 (http://www.copernicus-atmosphere.eu/). Model simulated specific humidity (q, kg/kg) was used to convert estimated CO_2 mixing ratios to dry air mixing ratios. CO_2 dry air mixing ratios are hereafter referred to CO_2 mixing ratios.

2.4 High-Resolution SOCE inventory development

The high-resolution SOCE inventory was constructed primarily from a pre-existing carbon monoxide (CO) inventory developed by the Pollutant Inventories and Reporting Division (PIRD) of ECCC as part of the 2010 Canadian Air Pollutant Emissions Inventory (APEI). The CO inventory is a comprehensive national anthropogenic inventory that includes emissions from area sources, point sources, on-road mobile sources and off-road mobile sources, including aircraft, locomotive and marine emissions for base year 2010 (Moran et al., 2015). This annual inventory at the provincial level compiled by PIRD was transformed into model-ready emissions files using the Sparse Matrix Operator Kernel Emissions (SMOKE, https://www.cmascenter.org/smoke/) emissions processing system for spatial allocation (distribution of non-point source emissions to 2.5 km x 2.5 km (roughly 0.02° x 0.02° resolution) using spatial surrogate fields) and temporal allocation (conversion of inventory annual emission rates into hourly values) (Moran et al., 2015). More detailed information about the CO

inventory compilation and subsequent processing has been provided elsewhere (Environment Canada, 2013; Moran et al., 2015; PIRD, 2016).

The objective of our work was to calculate CO_2 emissions based on this processed, model-ready CO inventory for Ontario grid cells using sector-specific emission ratios estimated by the Canadian National Inventory Report (NIR) (Environment Canada, 2012). Emission sources within each sector of the CO inventory are classified by SCC (Source Classification Code) and were converted to NFR (Nomenclature for Reporting) for accurate cross-reference with the NIR CO_2 and CO estimates. Provincial totals for CO_2 and CO are estimated based on the NFR sources that are included in the sector, producing the following sector-averaged CO_2:CO ratio:

$$CO_{2(sector,kt)} = CO_{(sector,kt)} * \frac{CO_{2(Ontario\ total,kt)}}{CO_{(Ontario\ total,kt)}} \qquad \text{Eq. (1)}$$

This sector-averaged CO_2:CO ratio is used to convert the APEI-based CO model-ready gridded emissions fields into CO_2 emissions fields at the same spatial and temporal resolution. A detailed outline of this conversion is presented for each sector in the following subsections. Unless otherwise noted, temporal allocation of emissions in each sector is based on estimates made available by SMOKE.

2.4.1 Area emissions

Area emissions are mostly small stationary sources that represent diffuse emissions that are not inventoried at the facility level. In the APEI CO inventory, the major emission sources in the Area sector include emissions from public electricity and heat production (1A1a), residential and commercial plants (1A4a and 1A4b), stationary agriculture/forestry/fishing (1A4c), iron and steel production (2C1), and pulp and paper (2D1). The NIR estimates an Ontario total from these (and other minor sources) of 23,455 kt CO_2 and 218.8 kt CO, producing a CO_2:CO ratio of 107.2 kt CO_2/kt

CO. This ratio was applied to every Area sector grid cell belonging to Ontario in the domain to convert sector CO emissions to CO_2 emissions.

2.4.2 Point emissions

Point emissions are stationary sources in which emissions exit through a stack or identified exhaust. In the APEI CO inventory, the major emission sources in the Point sector include public electricity and heat production (1A1a), stationary combustion in manufacturing industries and construction (1A2f), chemical industry (2B5a), pulp and paper (2D1), iron and steel production (2C1) and other metal production (2C5). Unlike the Area sector, we found that applying a single CO_2:CO ratio to every facility did not produce realistic CO_2 emissions due to the significant variability in combustion efficiency (and thus CO_2:CO ratio). Therefore, we used ECCC Facility Reported Data (Environment Canada, 2015) to identify the geocoded location and annual average CO_2:CO for 48 individual facilities in Ontario (Table S1) and applied the specific CO_2:CO ratios to the grid cells where the facilities were located. In addition, stack height of individual facilities were included in the emission model to optimize plume rise. All other point sources (minor facilities) were scaled by a sector average CO_2:CO ratio of 313.1 kt CO_2/kt CO, calculated from Ontario total CO_2 and CO point-source emissions from the NIR. Temporal allocation of emissions in the Point sector are based on facility level operating schedule data collected by ECCC.

2.4.3 On-road mobile emissions

On-road emissions include the emissions from any on-road vehicles (quantified by the Statistics Canada Canadian Vehicle Survey) (Environment Canada, 2013). In the APEI CO inventory, the major emission sources in the On-road sector includes gasoline and diesel-powered light- and heavy-duty vehicles (1A3b). The NIR estimates an Ontario total from these (and other minor on-road sources) of 44,458 kt CO_2 and 1508.3 kt CO, producing a CO_2:CO ratio of 29.5 kt CO_2/kt CO. This ratio was applied to every On-road grid cell belonging to Ontario in the domain to convert sector CO emissions to CO_2.

Temporal allocation of emissions in the On-road sector is estimated using data collected in the FEVER (Fast Evolution of Vehicle Emissions from Roadways) campaign in 2010 (Gordon et al., 2012a; Gordon et al., 2012b; Zhang et al., 2012).

2.4.4 Off-road mobile emissions

Off-road emissions include the emissions from any off-road vehicles that do not travel on designated roadways, including aircraft, all off-road engines, and locomotives. In the APEI CO inventory, the major emission sources in the Off-road sector include civil aviation (1A3a), railways (1A3c), and agriculture/forestry/fishing: off-road vehicles and other machinery (1A4c). Similar to the Point sector, we found that applying a single CO_2:CO ratio to every grid cell did not produce realistic CO_2 emissions for the two airports in the GTA, Pearson International Airport (PIA) and Billy Bishop Toronto City Airport (BBTCA). Therefore, we used air quality assessment reports compiled for each airport (RWDI AIR Inc., 2009; RWDI AIR Inc., 2013) to identify the geocoded location and facility-specific annual average CO_2:CO ratio. Sources of emissions from each airport include aircraft (landing and take-off cycles), auxiliary power units, ground support equipment, roadways, airside vehicles, parking lots, stationary sources and training fires; note that emissions from aircrafts in-transit between airports, which are injected in the free troposphere, have not been included in this inventory (Moran et al., 2015; RWDI AIR Inc., 2009). Based on these two reports, we applied a ratio of 175 kt CO_2/kt CO to the grid cell containing PIA and a ratio of 20 kt CO_2/kt CO to the grid cell containing BBTCA. All other off-road sources belonging to Ontario grid cells were scaled by a sector average CO_2:CO ratio of 7.2 kt CO_2/kt CO, calculated from NIR-reported Ontario total CO_2 and CO emissions.

2.4.5 Marine emissions

Commercial marine emissions include the emissions from any marine vessels travelling on the Great Lakes (quantified by the Statistics Canada *Shipping in Canada*) (Environment Canada, 2013). In the

APEI CO inventory, the major emission source in the Marine sector is national navigation (1A3d). The NIR estimates an Ontario total from this source of 729.2 CO_2 and 0.86 kt CO, producing a CO_2:CO ratio of 844.2 kt CO_2/kt CO. This ratio was applied to every marine grid cell in the domain to convert sector CO emissions to CO_2.

2.4.6 Residential and commercial emissions

Residential and commercial CO_2 emissions reflect on-site combustion of natural gas for electricity and heating, a source that we found was not included in the APEI CO inventory because of the high efficiency of the furnaces and resulting low CO emissions. To include the CO_2 emissions from these on-site furnaces, we used the Statistics Canada 2012 Report on Energy Supply and Demand to quantify the amount of natural gas consumed by residential and commercial buildings in Ontario, 7969.6 gigalitres (Gl) and 4895.7 Gl respectively (Statistics Canada, 2012a). We used an emission factor of 1879 g CO_2/m^3 natural gas combustion (Environment Canada, 2012) to estimate CO_2 emissions from residential and commercial on-site furnaces in Ontario to be 1.5 x 10^7 tonnes and 9.2 x 10^6 tonnes, respectively. These two emission totals were spatially allocated using a "capped-total dwelling" spatial surrogate developed by ECCC and temporally allocated using the SMOKE emissions processing system (Moran et al., 2015).

2.5 Biogenic flux

The net ecosystem exchange (NEE) fluxes used in our simulations were provided by the land surface component of the ECMWF forecasting system, C-TESSEL (Bousetta et al., 2013). Fluxes are extracted at the highest available resolutions, 15 x 15 km and 3 hour for January and February 2016 and 9 x 9 km and 3 hour for March. These data are interpolated in space and time to be consistent with our model resolution. With our main priority being understanding anthropogenic emissions in the GTA, we chose to analyze a period where the biogenic CO_2 flux is minimized and therefore this paper focuses on three winter months in 2016, January to March inclusive.

Atmos. Chem. Phys. Discuss., https://doi.org/10.5194/acp-2017-678
Manuscript under review for journal Atmos. Chem. Phys.
Discussion started: 26 July 2017

297 **3.0 Results and Discussion**

298 *3.1 The SOCE inventory*

299 Figure 1 displays the PanAm domain total anthropogenic CO_2 emissions estimated by the SOCE
300 inventory for the province of Ontario portion (~0.02° x 0.02°) and by the FFDAS v2 inventory (0.1° x
301 0.1°) (FFDAS, 2010) for the remainder of the domain. Regions of high emissions typically correspond
302 to population centers, for example the GTA in Ontario, Montreal and Quebec City in Quebec, and
303 Chicago, Boston and New York City (amongst others) in the USA. Emissions from highways and major
304 roadways are only clear in the province of Ontario (at higher spatial resolution) but industrial and
305 large scale area sources are evident across the entire domain.

306 The total CO_2 emissions can be separated into contributions from the seven sectors in the
307 province of Ontario described in *Sect. 2.4*. Figure 2 shows the anthropogenic CO_2 contributions from
308 the Area sector, Residential and Commercial sector, Point sector, Marine sector, On-road sector and
309 Off-road sector, focused on southern Ontario and the GTA. If we consider emissions from a domain
310 including the area solely around the GTA (indicated by the black-box in Figure 2a), the total CO_2
311 emissions estimated by the SOCE inventory is 94.8 Mt CO_2 per year, Table 2. Figures 2a and b display
312 the CO_2 emissions from the Area sector and from Residential and Commercial natural gas combustion
313 in southern Ontario. These two sectors combined represent the largest source of CO_2 in the black-
314 box area (41.6 Mt CO_2/year, contributing 43.9 % of the total). The majority of these emissions are
315 concentrated in the GTA and surrounding urban areas as a result of a significant portion of the
316 population (64 %) being reliant on natural gas for heat production (Statistics Canada, 2007; Statistics
317 Canada, 2012a). Figure 2c represents emissions from the Point sector, contributing 24.4 Mt CO_2/year,
318 25.7 % of the total. The largest point source emitters are located on the western shore of Lake Ontario
319 (Hamilton and surrounding areas) as this area is one of the most industrialized regions of the country
320 with intensive metal production activities. Figures 2d, e and f display CO_2 emissions from various

transportation sectors, Marine, On-road, and Off-road respectively, which together contribute more than 30 % of total CO_2 emissions in the area within the black box. While emissions from marine activity are minimal, those from On-road and Off-road sources are significant (25.0 % and 5.3 %, respectively), concentrating on the major highways connecting the various population centres of the GTA to the downtown core, as well as at PIA located within the city.

3.2 Comparison of the SOCE inventory with other inventories

The EDGAR v4.2 inventory estimates CO_2 emissions on an annual basis and by sector based on Selected Nomenclature for Air Pollution (SNAP) sub-sectors while FFDAS v2 provides hourly mean grid cell totals. Table 2 shows a comparison between the sectoral CO_2 estimates of the SOCE and EDGAR v4.2 inventories (SNAP sectors were grouped to correspond to SOCE sectors, Table S2) as well as the domain total estimated by the FFDAS v2 inventory for the area surrounding the GTA (the black-box area outlined in Figure 2a). There is a significant discrepancy between the CO_2 emissions estimated by the SOCE and EDGAR v4.2, inventories both in the relative sectoral contributions as well as domain total (percent difference >35 %). The largest sectoral discrepancies are in the Point and the On-road sectors, where the EDGAR v4.2 inventory estimates a contribution 1.9 and 1.7 times larger than that of the SOCE inventory, respectively. Figure 3 shows a comparison of the spatial distribution of the CO_2 inventory predicted by a) FFDAS v2, b) EDGAR v4.2, and c) SOCE (aggregated to 0.1^o x 0.1^o to match the resolution of EDGAR v4.2 and FFDAS v2) for the GTA area. Figure 3 reveals that the largest differences between the SOCE inventory and the EDGAR v4.2 inventory is the CO_2 emissions in the GTA; EDGAR v4.2 predicts much higher emissions in the GTA (in some grid cells, differences are an order of magnitude), particularly in the downtown core relative to the SOCE inventory.

Although there is no sectoral breakdown in the FFDAS v2 inventory, the domain total around the GTA can be compared to that of the SOCE inventory, Table 2. Unlike the comparison with the

345 EDGAR v4.2 inventory, there is a closer agreement between the FFDAS v2 inventory and the SOCE
346 inventory (difference of ~10 %). The comparison plots in Figure 3 show a good agreement of the
347 spatial variability of emissions in the GTA between the FFDAS v2 and SOCE inventories; however, the
348 gradient between urban and rural areas is not as sharp in the SOCE inventory as it is in the FFDAS v2
349 inventory. Furthermore, emissions along the western shore of Lake Ontario (Hamilton and the
350 surrounding areas) are predicted to be larger in the SOCE inventory relative to FFDAS v2. The FFDAS
351 v2 inventory was interpolated to 0.02 ° x 0.02° using a mass conservative interpolation scheme to
352 allow the production of a difference plot of the two inventories, SOCE minus FFDAS v2, shown in
353 Figure S1. The difference plot reveals the largest divergence between the inventories occurs in the
354 GTA and Ottawa, with the FFDAS v2 inventory estimating >1000 g CO_2/second (~30 kt CO_2/year)
355 more than the SOCE inventory in some grid cells. In addition to similar spatial variability, the FFDAS
356 v2 and SOCE inventories also have similar temporal variability. Figure S2 shows the diurnal profile
357 of estimated emissions from January-March for both the FFDAS v2 and SOCE inventories for the
358 black-box area in the PanAm domain. Both inventories allocate the highest emissions between 08:00
359 and 18:00 and the lowest emission between 00:00 and 5:00, however the amplitude of the diel cycle
360 is higher in SOCE, and emissions in the morning are as high as in the afternoon. FFDAS allocates a
361 relatively larger proportion of the emissions to the 15:00 – 19:00 period.

362 *3.3 Preliminary analyses using the SOCE, FFDAS v2 and EDGAR v4.2 inventories with FLEXPART*

363 To investigate the impact of the differing inventories on ambient mixing ratios, preliminary analyses
364 were run with footprints generated by the FLEXPART driven by GEM meteorology and products were
365 compared against the measured CO_2 gradient between the Downsview and TAO (43.7°N, 79.4°W, a
366 temporary site decommissioned in January 2016) stations in the year 2014. Observed gradients
367 ranged from +20 to -10 ppm. Figure S3 displays the measured and modelled CO_2 gradients. These
368 results show that when the EDGAR v4.2 inventory was used, simulated CO_2 gradients were

consistently overestimated by ~10-60 ppm relative to observations. Conversely, when the SOCE inventory was used, a higher level of agreement was obtained between simulated mixing ratios and measurements; however, none of the model simulations were able to capture times when the gradient was negative ($CO_{2,TAO} > CO_{2,Downsview}$), an effect we believe to be due to the TAO inlet being ~60 m above ground level and surrounded by many high-rise buildings creating canyon flows and turbulence which are not properly accounted for in GEM at this resolution. These factors contributed to the decommissioning of TAO in January 2016. The poor performance of our model system when using the EDGAR v4.2 inventory to simulate CO_2 mixing ratios was also found by a study quantifying on-road CO_2 emissions in Massachusetts, USA (Gately et al., 2013). In this study, EDGAR emission estimates were found to be significantly larger than any other inventory by as much as 9.3 million tons, or >33 %. The difference in estimates between the EDGAR v4.2 and the SOCE inventories is likely explained by their underlying differences in methodology. Being a global product and not specifically designed for mesoscale applications, the EDGAR v4.2 inventory estimates CO_2 emissions based on country-specific activity data and emission factors, however the spatial proxies used to disaggregate the data are not always optimal. A study performed by McDonald et al. (2014) showed that the use of road density as a spatial proxy for vehicle emissions in EDGAR v4.2 causes an overestimation of emissions in population centers (McDonald et al., 2014). Given the much larger emission estimates for On-road CO_2 from EDGAR v4.2 (Table 2), this also seems to be an issue in the GTA. Based on this large discrepancy, the EDGAR v4.2 inventory was not further used in this study and we focussed on the inventories developed for regional scale studies.

When similar preliminary analyses were run with FLEXPART footprints using the FFDAS v2 inventory, Figure S3, good agreement was observed with CO_2 gradients measured between the Downsview and TAO stations. We are confident that the enhanced measurement agreement between the FFDAS v2 and SOCE relative to EDGAR v4.2 is due to improved methodology; spatial allocation of emissions in FFDAS v2 is achieved through the use of satellite observations of nightlights from human

settlements from the U.S. Defense Meteorological Satellite Program Operational Linescan System (DMSP-OLS).

Beyond the differences in methodology for estimating and allocating emissions, it is important to note that the emissions reported in Table 2 by the FFDAS v2, SOCE and EDGAR v4.2 inventories also fundamentally differ in time period quantified. The emissions reported for both FFDAS v2 and the SOCE are based on emissions from three winter months (January-March 2010) extrapolated for the entire year. However, emissions from EDGAR v4.2 are annual averages of all twelve months of 2010. Since CO_2 emissions in the GTA are higher in the winter months relative to the summer months because of increased building and home heating, it is likely that the average annual estimates of SOCE and FFDAS v2 are slightly overestimated. This does not affect the relative agreement between SOCE and FFDAS v2 however it does further increase the divergence between the EDGAR v4.2 and SOCE and FFDAS v2 inventories. Following this and the improved agreement with observations, the FFDAS v2 inventory was used with the SOCE inventory for all subsequent modelling analyses.

3.4 Simulation of CO_2 mixing ratios in the Greater Toronto Area

We used the GEM-MACH CTM and the SOCE and FFDAS v2 inventories to simulate hourly CO_2 mixing ratios in the PanAm domain. The model framework was evaluated for a continuous three-month period, January-March 2016 using four sampling locations in the GTA, Figure 1 (note that measurements for the Hanlan's Point site were not available until January 14, 2016). Figure 4 displays afternoon (12:00-16:00 EST) measured and simulated CO_2 mixing ratios produced with the SOCE and FFDAS v2 inventories for the two emissions scenarios described in *Sect. 2.3* for the month of February (Figures S4 and S5 show the same figure for other months). We chose to present only afternoon data as this is the time of day when the mixed layer is likely to be the most well-developed; nighttime and morning data showed largest variations in observations as a result of the shallow

418 boundary layer causing surface emissions to accumulate within the lowest atmospheric layers
419 (Breon et al., 2015; Chan et al., 2008; Gerbig et al., 2008). During the night, atmospheric mixing ratios
420 are most sensitive to vertical mixing, an atmospheric process that is difficult to model for stable
421 boundary layers.

422 The time series comparisons at all four sites demonstrate the model's general ability to
423 capture variability in observations of CO_2, albeit with better skill for the Downsview and Egbert sites
424 (this is particularly clear when we look at model-measurement difference plots, Figure S6). The
425 model is able to capture many extreme events of mixing ratio increases and decreases, such as
426 February 11-14, 2016 at the Downsview site; however, some short time periods are poorly simulated,
427 such as January 21-23, 2016 at Hanlan's Point, when the model significantly overestimated measured
428 CO_2. Generally, mixing ratios simulated by the FFDAS v2 inventory are similar or larger than those
429 produced when the SOCE inventory is used, with differences most noticeable at the Downsview and
430 Hanlan's Point sites. This was expected as the difference plot shown in Figure S1 reveals that the
431 SOCE and FFDAS v2 inventories diverge the most in the GTA (where the Downsview and Hanlan's
432 Point sites are located) and are more similar in rural areas (where the Turkey Point and Egbert sites
433 are located).

434 Measured CO_2 mixing ratios have a typical diurnal pattern, in which mixing ratios are higher
435 at night and lower during the day, despite higher emissions during the day. This results from the daily
436 cycle of the mixed layer, which is shallow at night due to thermal stratification and deepens during
437 the day due to solar heating of the surface. Figure 5 displays the measured and modelled mean
438 diurnal profile of CO_2 at the four sites in our network using data from January-March, 2016 (note
439 difference in y-axis scale for urban vs. rural sites). At all four sites, the shapes of the modelled and
440 measured mixing ratios throughout the day agree very well, suggesting that the GEM meteorology in
441 our framework is capturing the diurnal variation in emissions and the boundary layer evolution. At

the Downsview site, there is a very strong agreement between the modelled and measured diurnal profiles when using the SOCE inventory, whereas the FFDAS v2 simulated profile largely overestimates mixing ratios, particularly at nighttime. This is consistent with the FFDAS inventory having larger emissions than the SOCE inventory during the night (Fig S2). At the Hanlan's Point site, a difference of ~ 5 ppm CO_2 is observed when using the SOCE inventory relative to measurements; however, similar to the Downsview site, the FFDAS v2 simulated profile has a larger difference of ~10 ppm CO_2. At both the Egbert and Turkey Point sites, the use of both inventories similarly overestimates the diurnal pattern of CO_2 mixing ratios by ~3-5 ppm, again likely a result of the similarities of these two inventories at these sites, Figure S1. At all four sites, it is possible that some of the biases that are observed in simulated CO_2 mixing ratios may arise from inaccuracies in the boundary CO_2 provided by MACC; this aspect was not, however, further explored in this study.

3.5 Quantifying model-measurement agreement

Figure 6 shows scatter plots of afternoon (12:00-16:00 EST) modelled versus measured CO_2 mixing ratios from January- March, 2016 at the four sites used in this study. The top row shows the correlation between measured and modelled mixing ratios using the SOCE inventory and the bottom row shows the correlation using the FFDAS v2 inventory. It is immediately clear that there is a stronger model-measurement correlation at the Downsview and Egbert sites ($R > 0.75$) relative to that of Hanlan's Point or Turkey Point ($R < 0.53$). The difficulty with accurately simulating CO_2 mixing ratios at Hanlan's Point and Turkey Point may arise from their proximity to shorelines, Hanlan's Point to Lake Ontario and Turkey Point to Lake Erie (see Figure 1). Differential heating of land versus water near these lakes creates pressure gradients driving unique circulation patterns (Burrows, 1991; Sills et al., 2011). These circulation patterns are difficult for models to capture and therefore may contribute to the relatively poor correlation observed at Hanlan's Point and Turkey Point.

It is also clear from Figure 6 that simulating CO_2 mixing ratios at the Egbert and Turkey Point sites using either the FFDAS v2 or the SOCE inventory results in similar performance, likely because the emissions estimated by the two inventories are similar in the vicinity of these two rural sites (see also Figure 5). However at both the Downsview and Hanlan's Point sites, using the SOCE inventory provided a slightly higher correlation and reduced RMSE and MB relative to using the FFDAS v2 inventory. The improvement by using the SOCE inventory is likely a result of both the improved spatial resolution (2.5 km versus 10 km), and therefore more accurate allocation of emissions to grid cells, and also a better estimation of emission magnitudes, as large differences are shown in Figures 3 and S1.

3.6 Sectoral contributions to simulated CO_2 mixing ratios

One of the major advantages of the SOCE inventory over the FFDAS v2 inventory is the availability of sectoral emission estimates. Figure 7 displays the sectoral percent contributions to diurnal CO_2 mixing ratio enhancements (calculated as local CO_2 mixing ratios above the MACC estimated background) for the Downsview station in February 2016 averaged by the day of week (Figures S7 and S8 displays the same for other months). This figure clearly demonstrates the importance of Area emissions (defined here as the sum of the Area + Residential natural gas combustion + Commercial natural gas combustion) to simulated CO_2 mixing ratios, reaching ~80 % contribution in the early morning and late evening, consistent with times when emissions from home heating are the dominant source of CO_2. Contributions from Area emissions decrease to ~35 % midday, which coincides with when emissions from other sources, such as On-road, gain importance. In the midday, emissions from the On-road sector can contribute ~50 %, which is consistent with transportation patterns of the times when the population is travelling to and from work and other activities. The relative contributions to CO_2 mixing ratios from point source emissions is quite variable during the course of a day and week, but generally seems to increase in the early morning and evening and can

contribute a significant portion of total CO_2 emissions (up to ~20 %). Figure 7 indicates that biogenic sources of CO_2 play a negligible role during January-March in the GTA. Recent studies, however, have shown the importance of the biospheric contribution (up to ~132-308 g CO_2 km^{-2} s^{-1}) to measured CO_2 in urban environments during the growing season (Decina et al., 2016). Therefore, this finding supports the importance of modelling CO_2 in the wintertime in cities like the GTA to avoid complications associated with biospheric contributions. The new ability to understand the sectoral contributions to CO_2 mixing ratios in the GTA and southern Ontario has implications from a policy perspective; with recent initiatives to curb CO_2 emissions, understanding from which sector the CO_2 is being emitted could be useful to assess how effective applied mitigation efforts have been or where to target future efforts. These efforts could be complemented by running simulations with additional tracers, such as carbon monoxide (CO), nitrogen oxides (NO_x), or stable carbon isotopes (^{12}C and ^{13}C) to gain further insight.

4.0 Conclusions

We presented the SOCE inventory for southern Ontario and the GTA, the first, to our knowledge, high-resolution CO_2 inventory for southern Ontario and for a Canadian metropolitan region. The SOCE inventory provides CO_2 emissions estimates at 2.5 km x 2.5 km spatial and hourly temporal resolution for seven sectors: Area, Residential natural gas combustion, Commercial natural gas combustion, Point, Marine, On-road and Off-road. When compared against two existing CO_2 inventories available for southern Ontario, the EDGAR v4.2 and the FFDAS v2 inventories, using FLEXPART footprints, the SOCE inventory had improved model-measurement agreement; FFDAS v2 agreed well with in situ measurements, but the EDGAR v4.2 inventory systematically overestimated mixing ratios. We developed a model framework using the GEM-MACH chemistry-transport model on a high-resolution 2.5 km x 2.5 km grid coupled to the SOCE and FFDAS v2 inventories for anthropogenic CO_2 emissions and C-TESSEL for biogenic CO_2 fluxes. We compared output simulations

513 to observations made at four stations across southern Ontario and for three winter months, January
514 – March, 2016. Model-measurement agreement was strong in the afternoon using both
515 anthropogenic inventories, particularly at the Downsview and Egbert sites. Difficulty in capturing
516 mixing ratios at the Hanlan's Point and Turkey Point sites was hypothesized to be a result of their
517 close proximity to shorelines (Lake Ontario and Lake Erie, respectively) and the model's inability to
518 capture the unique circulation patterns that occur in those environments. Generally, across all
519 stations and months, simulations using the SOCE inventory resulted in higher model-measurement
520 agreement than those using the FFDAS v2 inventory, quantified using R, RMSE and mean bias. In
521 addition to improved agreement, the primary advantage of the SOCE inventory over the FFDAS v2
522 inventory is the sectoral breakdown of emissions; using average day of week diurnal mixing ratio
523 enhancements, we were able to demonstrate that emissions from area sources can contribute >80 %
524 of CO_2 mixing ratio enhancements in the early morning and evening with on-road sources
525 contributing >50 % midday. The applications of the SOCE inventory will likely show future utility in
526 understanding the impacts of CO_2 reduction efforts in southern Ontario and identify target areas
527 requiring further improvement.

528 *Author Contributions*

529 The SOCE inventory was prepared by Stephanie C. Pugliese, with critical input from Felix Vogel and
530 Jennifer Murphy. The CO inventory which the SOCE inventory is based upon was provided by Mike
531 Moran, Junhua Zhang and Qiong Zheng. The GEM-MACH modelling analyses were performed by
532 Shuzhan Ren and Craig Stroud. The ambient CO_2 data were collected by Douglas Worthy and his team
533 at Environment and Climate Change Canada. The MACC and C-TESSEL products used in our model
534 simulations were provided by Gregoire Broquet. The data was analyzed and interpreted for
535 publication by Stephanie C. Pugliese. This manuscript was written by Stephanie C. Pugliese, with
536 critical input from Jennifer Murphy, Felix Vogel and Mike Moran.

Acknowledgements

The authors are thankful to Robert Kessler, Michelle Ernst, Lauriant Giroux, Senen Racki and Lin Huang for their efforts collecting the $^{12}CO_2$ and $^{13}CO_2$ measurements at Environment and Climate Change Canada. They would also like to thank Elton Chan for providing the FLEXPART footprints and for Pegah Baratzadeh for help creating the SOCE inventory.

References

Bousetta, S., Balsamo, G., Beljaars, A., Panareda, A. A., Calvet, J. C., Jacobs, C., van den Hurk, B., Viterbo, P., Lafont, S., Dutra, E., Jarlan, L., Balzarolo, M., Papale, D., and van der Werf, G. (2013). Natural Land Carbon Dioxide Exchanges in the ECMWF Integrated Forecasting System: Implementation and Offline Validation. Journal of Geophysical Research: Atmospheres, 118, 5923-5946.

Breon, F. M., Broquet, G., Puygrenier, V., Chevallier, F., Xueref-Remy, I., Ramonet, M., Dieudonne, E., Lopez, M., Schmidt, M., Perrussel, O., and Cias, P. (2015). An Attempt at Estimating Paris Area CO_2 Emissions from Atmospheric Concentration Measurements. Atmospheric Chemistry and Physics, 15(1707), 1724.

Burrows, W. R. (1991). Objective Guidance for 0–24-Hour and 24–48-Hour Mesoscale Forecasts of Lake-Effect Snow using CART. American Meteorological Society, 6, 357-378.

C40 Cities. (2016). C40 Cities: Global Leadership on Climate Change. Retrieved 10/12, 2016, from http://www.c40.org/cities/toronto

Chan, D., Ishizawa, M., Higuchi, K., Maksyutov, S., and Chen, J. (2008). Seasonal CO_2 Rectifier Effect and Large-Scale Extratropical Atmospheric Transport. Journal of Geophysical Research, 113(D17309) doi:doi:10.1029/2007JD009443

Côté, J., Desmarais, J, Gravel, S., Méthot, A., Patoine, A., Roch, M., and and Staniforth, A. (1998b). The Operational CMC/MRB Global Environment Multiscale (GEM) Model. Part II: Results. Monthly Weather Review, 126, 1397-1418.

563 Côté, J., Gravel, S., Méthot, A., Patoine, A., Roch, M., and and Staniforth, A. (1998a). The Operational
564 CMC/MRB Global Environmental Multiscale (GEM) Model. Part 1: Design Considerations and
565 Formulation. Monthly Weather Review, 126, 1373-1395.

566 Decina, S. M., Hutyra, L. R., Gately, C. K., Getson, J. M., Reinmann, A. B., Short Gianotti, A. G., and
567 Templer, P. H. (2016). Soil Respiration Contributes Substantially to Urban Carbon Fluxes in the
568 Greater Boston Area. Environmental Pollution, 212, 433-439.

569 EDGAR. (2010). Emission Database for Global Atmospheric Research Release Version 4.2 of the
570 European Commission. Joint Research Centre (JRC)/Netherlands Environmental
571 Assessment Agency (PBL). Retrieved 06/29, 2016, from http://edgar.jrc.ec.europa.eu

572 Environment Canada. (2011). Canadian Greenhouse Gas Measurement Program. Retrieved 10/07,
573 2016, from https://www.ec.gc.ca/mges-ghgm/

574 Environment Canada. (2012). National Inventory Report 1990-2010: Greenhouse Gas Sources and
575 Sinks in Canada. Retrieved 10/07, 2016, from http://www.ec.gc.ca/ges-ghg/

576 Environment Canada. (2013). Manual for the Compilation of Canada's 2010 Air Pollutant Emissions.
577 Catalogue no. En14-87/2013E-PDF. Retrieved 10/07, 2016, from
578 http://www.ec.gc.ca/Publications/default.asp?lang=En&xml=8A08B403-C85E-4612-A958-
579 3F24446A61DB

580 Environment Canada. (2015). Reported Facility Greenhouse Gas Data. Retrieved 10/07, 2016, from
581 http://www.ec.gc.ca/ges-ghg/donnees-data/index.cfm?lang=En

582 FFDAS. (2010). Fossil Fuel Data Assimilation System (FFDAS). Retrieved 06/29, 2016, from
583 http://hpcg.purdue.edu/FFDAS/

584 Framework for Public Review and Engagement. (2007). Change is in the Air: Toronto's
585 Commitment to an Environmentally Sustainable Future. Retrieved 10/12, 2016, from
586 www.toronto.ca/legdocs/mmis/2007/ex/bgrd/backgroundfile-2428.pdf

587 Gately, C. K., Hutyra, L. R., Sue Wing, I., and Brondfield, M. N. (2013). A Bottom-Up Approach to on-
588 Road CO_2 Emissions Estimates: Improved Spatial Accuracy and Applications for Regional
589 Planning. Environmental Science and Technology, 47, 2423-2430.

590 Gerbig, C., Korner, S., and Lin, J. C. (2008). Vertical Mixing in Atmospheric Tracer Transport Models:
591 Error Characterization and Propagation. Atmospheric Chemistry and Physics, 8, 591-602.

592 Gong, W., Makar, P. A., Zhang, J., Milbrandt, J., Gravel, S., Hayden, K. L., Macdonald, A. M., and Leaitch,
593 W. R. (2015). Modelling Aerosol-Cloud-Meteorology Interaction: A Case Study with a Fully
594 Coupled Air Quality Model (GEM-MACH). Atmospheric Environment, 115, 695-715.

595 Gordon, M., Staebler, R. M., Liggio, J., Li, S., Wentzell, J., Lu, G., Lee, P., and Brook, J. R. (2012a).
596 Measured and Modeled Variation in Pollutant Concentration Near Roadways. Atmopsheric
597 Environment, 57, 138-145.

598 Gordon, M., Staebler, R. M., Liggio, J., Makar, P., Li, S., Wentzell, J., Lu, G., Lee, P., and Brook, J. R.
599 (2012b). Measurements of Enhanced Turbulent Mixing Near Highways. Journal of Applied
600 Meteorology and Climatology, 51, 1618-1632.

601 Gurney, K. R., Mendoza, D. L., Zhou, Y., Fischer, M. L., Miller, C. C., Geethakumar, S., and De La Rue du
602 Can, S. (2009). High Resolution Fossil Fuel Combustion CO_2 Emission Fluxes for the United
603 States. Environmental Science and Technology, 43, 5535-5541.

Gurney, K. R., Razlivanvov, I., Song, Y., Zhou, Y., Benes, B., and Abdul-Massih, M. (2012). Quantification of Fossil Fuel CO_2 Emissions on the Building/Street Scale for a Large U.S. City. Environmental Science and Technology, 46(21), 12194-12202.

IPCC-WG3. (2014). Climate Change 2014: Mitigation of Climate Change.Working Group III Contribution to the Fifth Assessment Report of the Intergovernmental Panel on Climate Change. Retrieved 10/12, 2016, from http://www.ipcc.ch/report/ar5/wg3/

McDonald, B. C., McBride, Z. C., Martin, E. W., and Harley, R. A. (2014). High-Resolution Mapping of Motor Vehicle Carbon Dioxide Emissions. Journal of Geophysical Research: Atmospheres, 119, 5283-5298.

Miller, S. M., and Michalak, A. M. (2016). Constraining Sector-Specific CO_2 and CH_4 Emissions in the United States. Atmospheric Chemistry and Physics Dicsussions, doi:doi:10.5194/acp-2016-643

Moran, M., Zheng, Q., Zhang, J. and Pavlovic, R. (2015). RAQDPS Version 013: Upgrades to the CMC Operational Regional Air Quality Deterministic Prediction System Released in June 2015. Retrieved 10/07, 2016, from http://collaboration.cmc.ec.gc.ca/cmc/cmoi/product_guide/docs/lib/op_systems/doc_opchanges/Technical_Note_GEM-MACH10_v1.5.3+SET2.1.1_Emissions_9Nov2015.pdf

Moran, M. D., Dastoor, A., & Morneau, G. (2013). Long-range transport of air pollutants and regional and global AQ modelling. In E. Taylor, & A. McMillan (Eds.), Air Quality Management - Canadian Perspectives on a Global Issue (pp. 69-98) Springer.

Ontario. (2016). Ontario's Five Year Climate Change Action Plan 2016-2020. Retrieved 09/14, 2016, from https://www.ontario.ca/page/climate-change-action-plan

625 Patarasuk, R., Gurkey, K. R., O'Keeffe, D., Song, Y., Huang, J., Rao, P., Buchert, M., Lin, J. C., Mendoza,
626 D., and Ehleringer, J. R. (2016). Urban High-Resolution Fossil Fuel CO_2 Emissions Quantification
627 and Exploration of Emission Drivers for Potential Policy Applications. Urban Ecosytems, 19(3),
628 1013-1039.

629 Pavlovic, R., Chen, J., Anderson, K., Moran, M. D., Beaulieu, P., Davignon, D., and Cousineau, S. (2016).
630 The FireWork Air Quality Forecast System with Near-Real-Time Biomass Burning Emissions:
631 Recent Developments and Evaluation of Performance for the 2015 North American Wildfire
632 Season. Journal of the Air and Waste Management Association, 66(9), 819-841.

633 Pillai, D., Gerbig, C., Ahmadov, R., Rodenbeck, C., Kretschmer, R., Koch, T., Thompson, R., Neininger,
634 B., and Lavrie, J. V. (2011). High Resolution Simulations of Atmospheric CO_2 Over Complex
635 Terrain - Representing the Ochsenkopf Mountain Tall Tower. Atmospheric Chemistry and
636 Physics, 11, 7445-7464.

637 PIRD. (2016). Air Pollutant Emission Inventory Report (APEIR) 1990-2014. Retrieved 10/07, 2016,
638 from http://www.ec.gc.ca/Air/89ED82E9-CA92-424E-9FD1-
639 C57235A04CE0/Air%20Pollutant%20Emission%20Inventory%20Report%201990-2014.pdf

640 RWDI AIR Inc. (2009). 2007 emissions inventory Toronto Pearson International Airport, Toronto,
641 Ontario.

642 RWDI AIR Inc. (2013). Billy Bishop Toronto City Airport (BBTCA) final report: Air quality review.

643 Sills, D., Brook, J., Levy, I., Makar, P., Zhang, J., and Taylor, P. (2011). Lake Breezes in the Southern
644 Great Lakes Region and their Influence during BAQS-Met 2007. Atmospheric Chemistry and
645 Physics, 11, 7955-7973.

646 Statistics Canada. (2007). Households and the Environment: Energy Use. Retrieved 12/04, 2012,
647 from http://www.statcan.gc.ca/pub/11-526-s/2010001/t002-eng.pdf

648 Statistics Canada. (2009). Table 3.4: Total and Urban Land Area, 1996, 2001 (Modified) and 2006.
649 Retrieved 10/12, 2016, from http://www.statcan.gc.ca/pub/92f0138m/2008001/t/4054949-
650 eng.htm

651 Statistics Canada. (2011). Population, Urban and Rural, by Province and Territory (Canada).
652 Retrieved 10/12, 2016, from http://www.statcan.gc.ca/tables-tableaux/sum-
653 som/l01/cst01/demo62a-eng.htm

654 Statistics Canada. (2012a). Report on Energy Supply and Demand. Retrieved 12/04, 2015, from
655 http://www.statcan.gc.ca/pub/57-003-x/2015001/t037-eng.pdf

656 Statistics Canada. (2012b). Focus on Geography Series, 2011 Census. Statistics Canada Catalogue no.
657 98-310-XWE2011004. Retrieved 08/13, 2013, from https://www12.statcan.gc.ca/census-
658 recensement/2011/as-sa/fogs-spg/Facts-cma-eng.cfm?LANG=Eng&GK=CMA&GC=535

659 Talbot, D., Moran, M. D., Bouchet, V., Creview, L., Menard, S., Kallur, A., & and the GEM-MACH Team.
660 (2008). Development of a new Canadian operational air quality forecast model. In C. Borrego,
661 & A. I. Miranda (Eds.), Air Pollution Modeling and its Application XIX (pp. 470-478) Springer
662 Science and Business Media.

663 Wang, R., Tao, S., Ciais, P., Shen, H. Z., Huang, Y., Chen, H., Shen, G. F., Wang, B., Li, W., Zhang, Y. Y., Lu,
664 Y., Zhu, D., Chen, Y. C., Liu, X. P., Wang, W. T., Wang, X. L., Liu, W. X., Li, B. G., and and Piao, S. L.
665 (2013). High-Resolution Mapping of Combustion Processes and Implications for CO_2
666 Emissions. Atmospheric Chemistry and Physics, 13, 5189-5203.

667 WHO. (2015). Global Health Observatory (GHO) Data: Urban Population Growth. Retrieved 2/3,
668 2015, from
669 http://www.who.int/gho/urban_health/situation_trends/urban_population_growth_text/en/

670 Worthy, D. E., Platt, A., Kessler, R., Ernst, M., Audette, C., & Racki, S. (2005). An update on the
671 Canadian GHG measurement program, in: Report of the 12th WMO/IAEA meeting of experts on
672 carbon dioxide concentration related tracer measurement techniques. (No. 162). Toronto,
673 Canada: World Meteorological Organization Atmosphere Watch.

674 Zhang, J., Zheng, Q., Moran, M. D., Gordon, M., Liggio, J., Pakar, P., & Stroud, C. (2012). Improvements
675 to SMOKE processing of Canadian on-road mobile emissions. Toronto, Canada.

676 Zhao, Y., Nielsen, C. P., and McElroy, M. B. (2012). China's CO_2 Emissions Estimated from the Bottom
677 Up: Recent Trends, Spatial Distributions and Quantification of Uncertainties. Atmospheric
678 Environment, 59, 214-223.

679

680

Atmos. Chem. Phys. Discuss., https://doi.org/10.5194/acp-2017-678
Manuscript under review for journal Atmos. Chem. Phys.
Discussion started: 26 July 2017

Atmospheric Chemistry and Physics Discussions

Table 1: **Summary of atmospheric measurement programs in Southern Canada operated by Environment and Climate Change Canada**

Start Date	Site Name	Coordinates	Elevation (asl)	Intake Height	In-situ Instrumentation
March, 2005	Egbert	44.231037N, 79.783834W	251m	3m, 25m*	NDIR
November, 2010	Downsview	43.780491N, 79.468010W	198m	20m	NDIR
November, 2012	Turkey Point	42.635368N, 80.557659W	231m	35m	CRDS
June, 2014	Hanlan's Point	43.612201N 79.388705W	87m	10m	CRDS

* At Egbert, a 25 m tower was installed in March 9, 2009
NDIR = Non-dispersive infrared
CRDS = cavity ring-down spectroscopy

Atmos. Chem. Phys. Discuss., https://doi.org/10.5194/acp-2017-678
Manuscript under review for journal Atmos. Chem. Phys.
Discussion started: 26 July 2017

Atmospheric Chemistry and Physics Discussions

688 **Table 2: Anthropogenic CO_2 emissions for the year 2010 in the black-box area (shown in**
689 **Figure 2a) by sector. Values in parentheses indicate the percentage contribution of the**
690 **sector to the total CO_2 emissions in the black-box area.**

Sector	FFDAS v2‡ CO_2 Inventory (Mt CO_2/year)	EDGAR v4.2# CO_2 Inventory (Mt CO_2/year)	SOCE CO_2 Inventory (Mt CO_2/year)
Area*	-	46.2 (33.9 %)	41.6 (43.9 %)
Point	-	45.9 (33.7 %)	24.4 (25.7 %)
Marine	-	0.12 (0.10 %)	0.10 (0.10 %)
On-road	-	41.2 (30.2 %)	23.7 (25.0 %)
Off-road	-	2.95 (2.2 %)	5.01 (5.3 %)
Total	104.8	136.4	94.8

691 *Area sector represents the summation of Area + Residential + Commercial natural gas combustion.
692 #The EDGAR inventory v4.2 can be found at http://edgar.jrc.ec.europa.eu.
693 ‡The FFDAS v2 inventory can be found at http://hpcg.purdue.edu/FFDAS/.
694

695

696

Atmos. Chem. Phys. Discuss., https://doi.org/10.5194/acp-2017-678
Manuscript under review for journal Atmos. Chem. Phys.
Discussion started: 26 July 2017

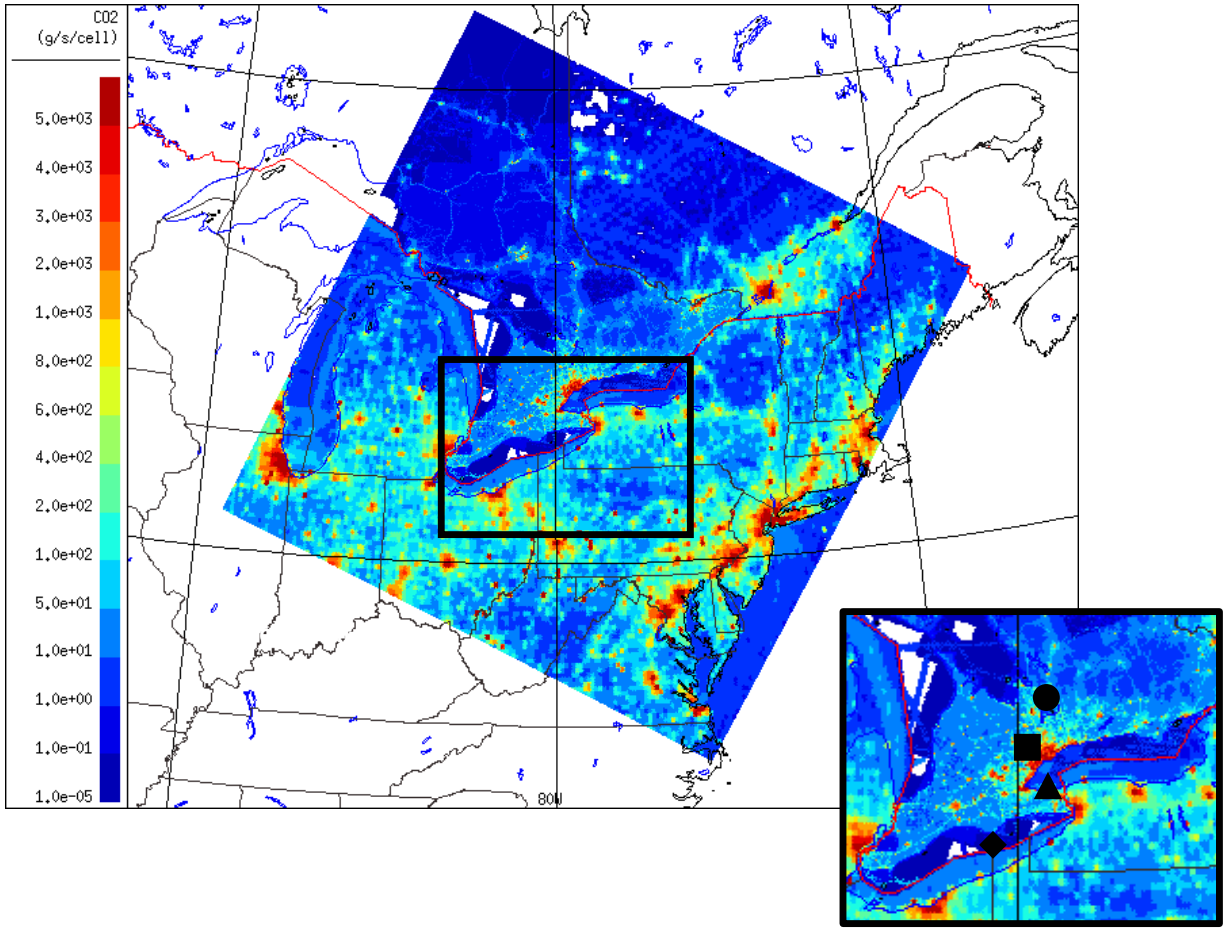

Figure 1: Total anthropogenic CO_2 emissions for a weekday in February 2010 estimated by the SOCE inventory for the province of Ontario and by the FFDAS v2 inventory for the remainder of the GEM-MACH PanAm domain. Locations of in-situ measurements of CO_2 in the Southern Ontario GHG Network are shown in the inset (Downsview = square, Egbert = circle, Hanlan's Point = triangle, Turkey Point = diamond). The Downsview and Hanlan's Point sites are both located in the GTA. Units: g CO_2/second/grid cell.

Atmos. Chem. Phys. Discuss., https://doi.org/10.5194/acp-2017-678
Manuscript under review for journal Atmos. Chem. Phys.
Discussion started: 26 July 2017

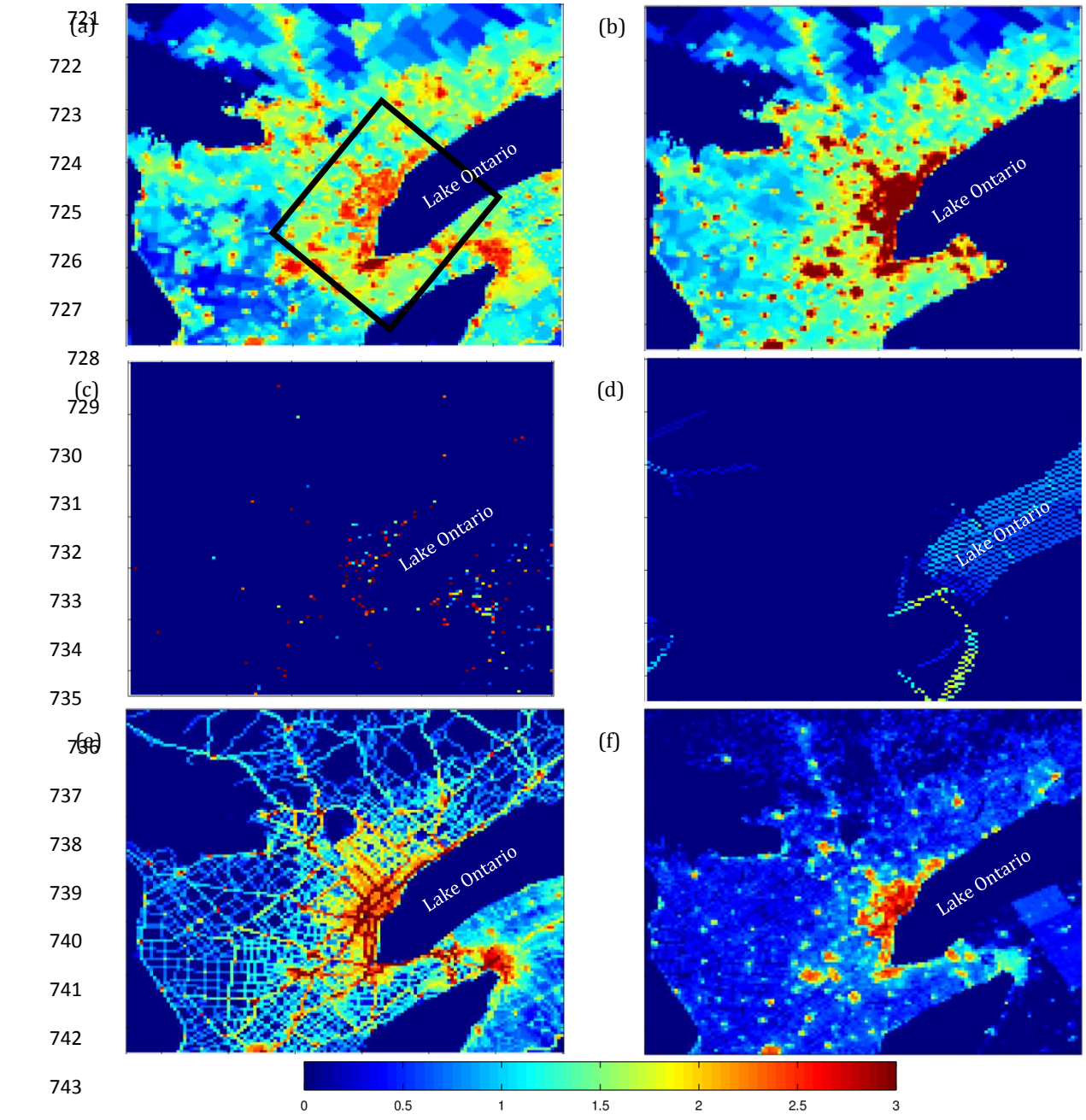

Figure 2: Anthropogenic CO_2 emissions for a weekday in February 2010 in southern Ontario. Emissions are estimated by the SOCE inventory for the (a) Area sector; (b) sum of the Residential and Commercial sectors; (c) Point sector; (d) Marine sector; (e) On-road sector; (f) Off-road sector. Units: $\log_{10}$(g CO_2/second/grid cell).

Atmos. Chem. Phys. Discuss., https://doi.org/10.5194/acp-2017-678
Manuscript under review for journal Atmos. Chem. Phys.
Discussion started: 26 July 2017

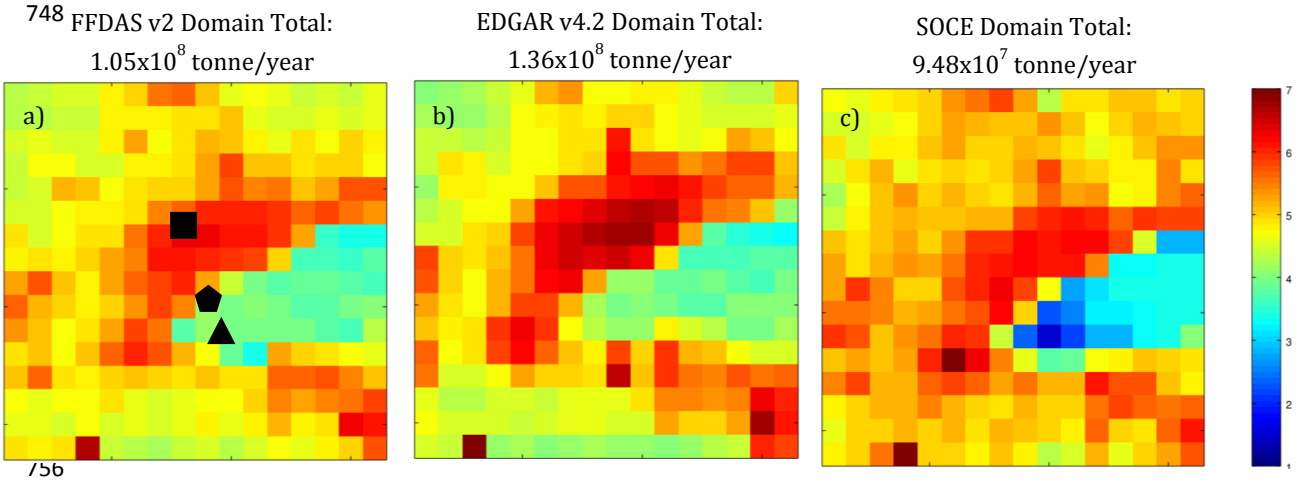

Figure 3: Comparison of spatial distribution of annual CO_2 emissions inventories for the black-box area (shown in Figure 2a) at 0.1° x 0.1° resolution. Panel a) shows the FFDAS v2 inventory estimate, Panel b) shows the EDGAR v4.2 inventory estimate and Panel c) shows the SOCE inventory estimate. Units: $\log_{10}$(tonne CO_2/year/grid cell). Domain totals are shown on top of each panel and locations of in-situ measurements of CO_2 for three stations in the Southern Ontario GHG Network are shown on Panel a (Downsview = square, Hanlan's Point = triangle, TAO = pentagon). The other two stations, Egbert and Turkey Point, are located outside this area.

Atmos. Chem. Phys. Discuss., https://doi.org/10.5194/acp-2017-678
Manuscript under review for journal Atmos. Chem. Phys.
Discussion started: 26 July 2017

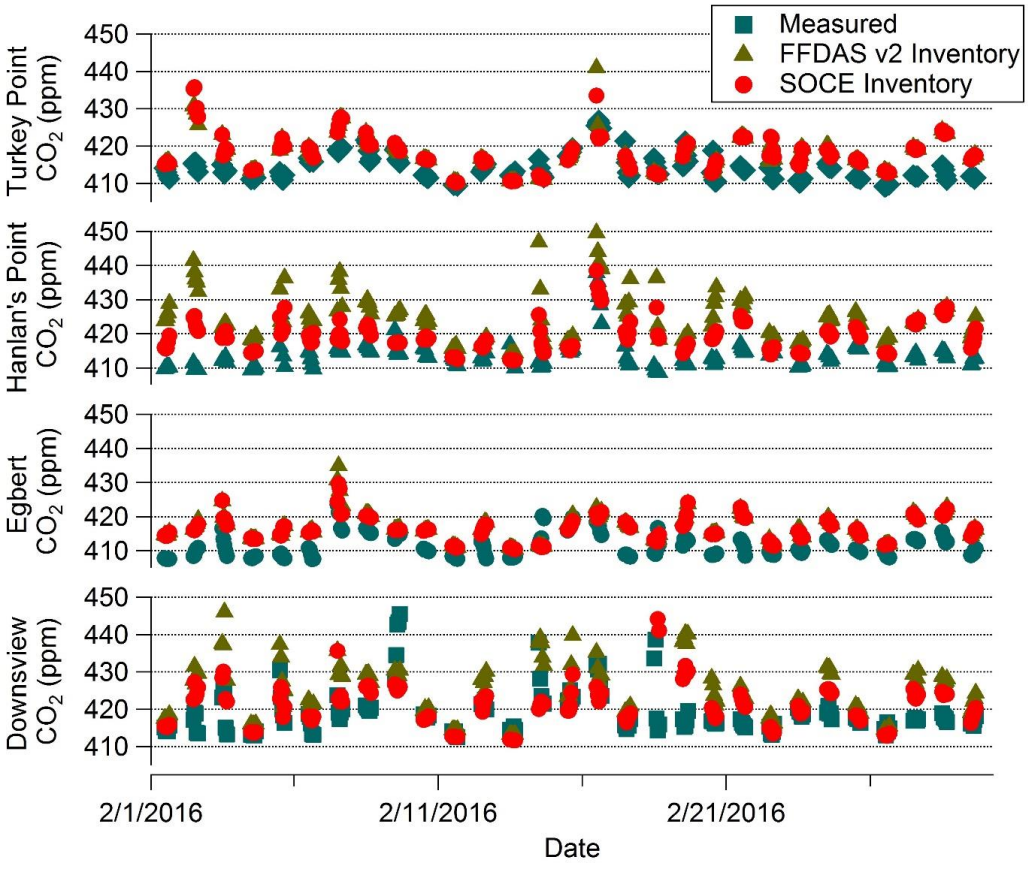

766

767 **Figure 4: Time series of measured (blue) and modelled February afternoon (12:00-16:00 EST)**
768 **CO_2 mixing ratios for the four sites used in this study. The red and gold markers are the**
769 **modelled mixing ratios when using the SOCE CO_2 inventory and the FFDAS v2 inventory,**
770 **respectively.**

771

Atmos. Chem. Phys. Discuss., https://doi.org/10.5194/acp-2017-678
Manuscript under review for journal Atmos. Chem. Phys.
Discussion started: 26 July 2017

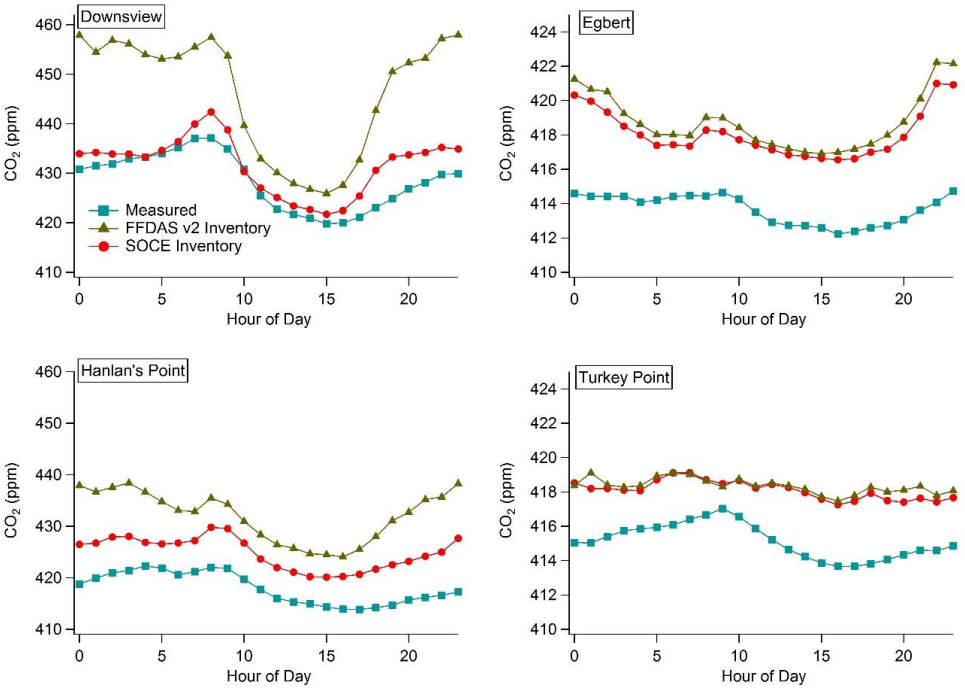

Figure 5: Time series of mean measured (blue) and modelled diurnal CO_2 mixing ratios at the four sites considered in this study for January – March 2016. The red and gold markers are the modelled diurnal mixing ratios when using the SOCE CO_2 inventory and the FFDAS v2 inventory, respectively. Note the difference in scale for urban and rural sites.

Atmos. Chem. Phys. Discuss., https://doi.org/10.5194/acp-2017-678
Manuscript under review for journal Atmos. Chem. Phys.
Discussion started: 26 July 2017

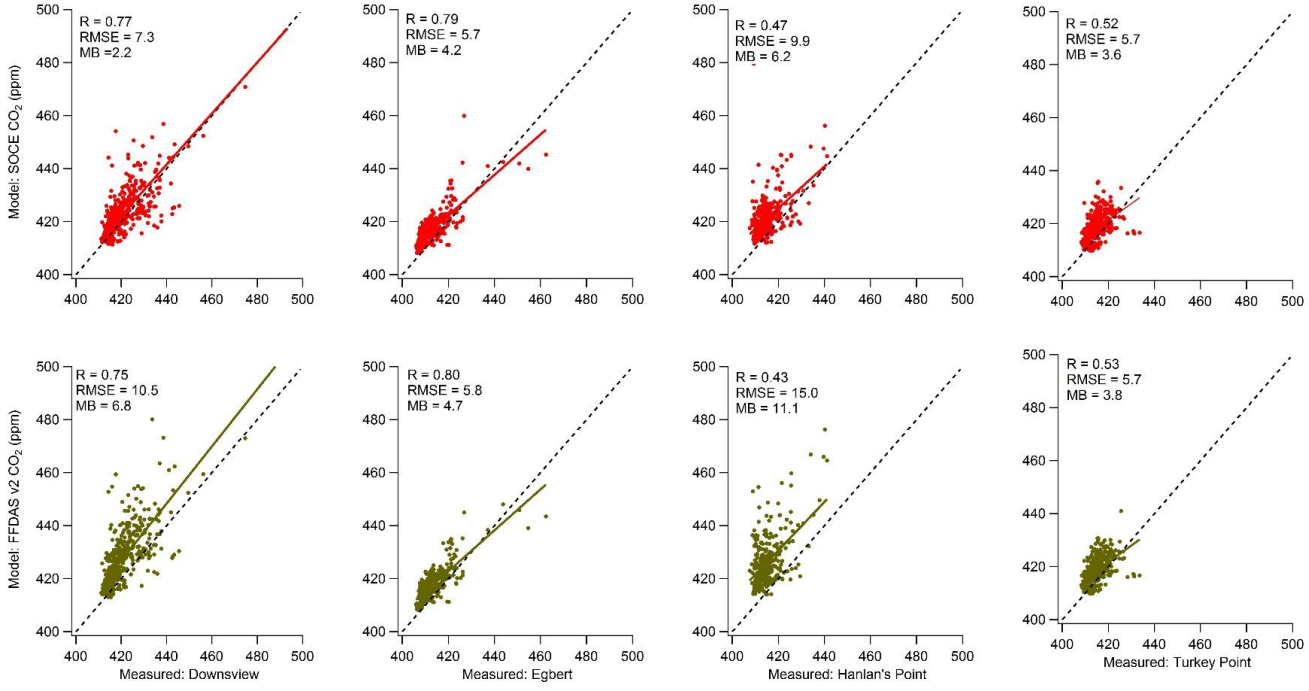

Figure 6: Scatter plot of the modelled and measured afternoon (12:00-16:00 EST) CO_2 mixing ratios from January-March, 2016 at the four monitoring stations used in this study. The top and bottom panels show measurement-model correlation when the SOCE inventory and the FFDAS v2 inventory were used, respectively. The model vs. measurement Correlation Coefficient (R), root mean square error (RMSE) and mean bias (MB) (units: ppm) are provided within each panel. Solid lines are the standard major axis regression lines and dashed lines are 1:1 lines shown for reference.

Atmos. Chem. Phys. Discuss., https://doi.org/10.5194/acp-2017-678
Manuscript under review for journal Atmos. Chem. Phys.
Discussion started: 26 July 2017

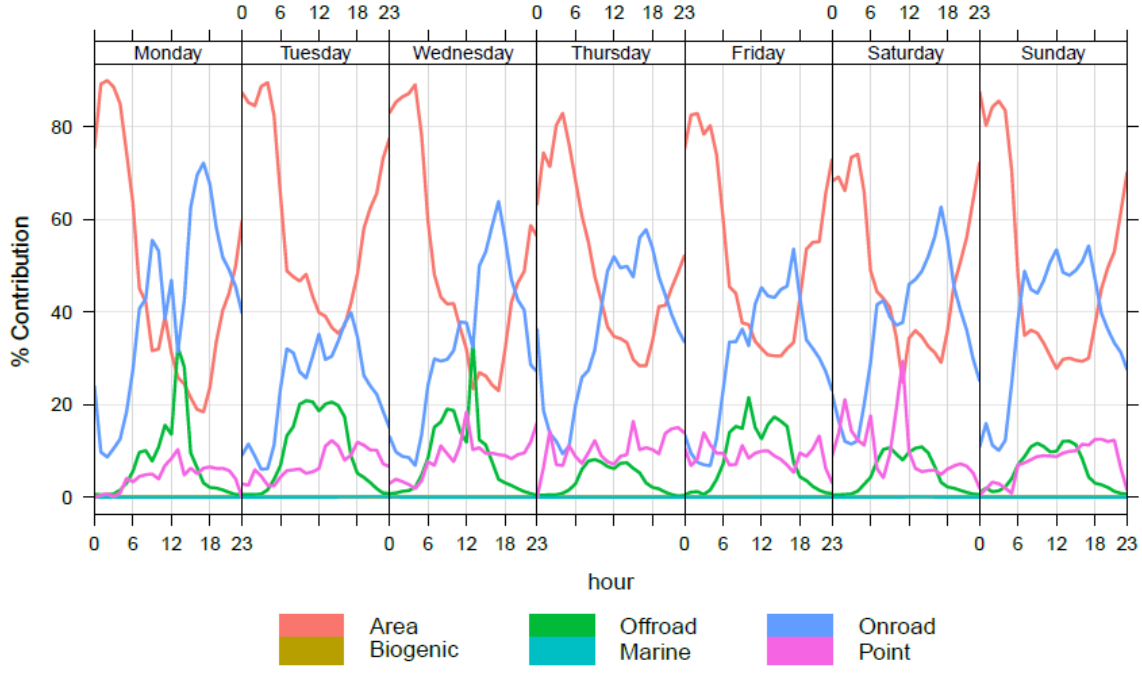

Figure 7: Modelled sectoral percent contributions to diurnal local CO_2 enhancement for February 2016 at Downsview averaged by day of week. Note: Area = Area + Residential natural gas combustion + Commercial natural gas combustion. (Time zone is EST).